

# Excellence in Chemistry Research

## Announcing our new flagship journal

- Gold Open Access
- Publishing charges waived
- Preprints welcome
- Edited by active scientists



## Meet the Editors of *ChemistryEurope*



**Luisa De Cola**

Università degli Studi  
di Milano Statale, Italy



**Ive Hermans**

University of  
Wisconsin-Madison, USA



**Ken Tanaka**

Tokyo Institute of  
Technology, Japan

Special  
Collection

# Covalently Modified Kevlar Fabric Incorporating Graphene Oxide with Enhanced Antibacterial Properties and Preserved Strength

Ruben Canton-Vitoria,<sup>\*[a]</sup> Nikolaos Heliopoulos,<sup>[b]</sup> Nikos Boukos,<sup>[c]</sup> Sozon Vasilakos,<sup>[d]</sup> Dionysios Siamidis,<sup>[d]</sup> Kostas Stamatakis,<sup>[e]</sup> and Nikos Tagmatarchis<sup>\*[a]</sup>

Dedicated to Prof. Maurizio Prato on the occasion of his 70<sup>th</sup> birthday.

This work describes a multi-step modification process for the covalent transformation of Kevlar fabric en route to the incorporation of graphene oxide (GO) nanosheets. Spectroscopic, thermal and microscopy imaging techniques have been employed to follow step-by-step the modification of Kevlar and the formation of the corresponding Kevlar-GO hybrid fabric. The level of Kevlar's functionalization can be controlled with the nitration time, the first reaction in the multi-sequence organic transformations, for obtaining the hybrid fabric with a content of GO up to 30%. Most importantly, the covalent post-modification of Kevlar does not occur in the expense of the other excellent mechanical properties of the fabric. Under

optimal conditions, the Kevlar-GO hybrid fabric shows a 20% enhancement of the ultimate strength. Notably, when the Kevlar-GO hybrid fabric was exposed to cyanobacterial *Synechococcus* the bacteria growth was fully inhibited. Overall, the covalently modified fabric demonstrated significant antibacterial behavior, excellent strength and stability under common processes. Due to its simplicity, the methodology presented in this work not only promises to result in a standard procedure to functionalize the *mer* units of Kevlar with a variety of chemicals and nanomaterials but it can be also extended for the modification and hybridization of other fabrics.

## Introduction

Aramid fibers of Kevlar are extremely important in a wide range of applications like body armors, composites of aircrafts or radiation shielding.<sup>[1–3]</sup> The chemical structure of Kevlar corresponds to molecular chains of poly(paraphenylene terephthalamide), abbreviated as PPTA, interconnected by a plethora of hydrogen bonds,  $\pi$ - $\pi$  stacking interactions and van der Waals forces.<sup>[4,5]</sup> As a result, the effect of these three type of interactions is to provide excellent properties to Kevlar fibers, including mechanical strength with an ultimate tensile strength superior to 3.6 GPa and a Young's modulus of 90 GPa.<sup>[6,7]</sup> The strength properties of Kevlar remains stable over the time, for example, fibers of Kevlar were stressed with a tension of 1.8 GPa, producing a variation of the strain of only 13% after 1000 days.<sup>[8]</sup> In addition, Kevlar is chemically robust under very aggressive conditions and has excellent thermal stability for example at 500 °C or more in the presence of air.<sup>[9]</sup>

In previous years, Kevlar has been functionalized with different nanomaterials, with main aim of the reinforcement of its mechanical properties. For example, the tensile strength and Young's modulus of Kevlar nanofibers were found boosted by 85 and 76%, respectively, after the addition of only 0.75% of graphene oxide.<sup>[10]</sup> In addition, nanomaterials can enhance the properties of fabrics acting as flame retardant, UV light shield and water or bacteria repellent.<sup>[11]</sup> For example, the hydrophilicity of Kevlar was also enhanced, evidenced by the decrease of the water contact angle from 87 to 60°. <sup>[10]</sup> Similarly, interactions of Kevlar with carbon nanotubes (CNTs) resulted in

[a] Dr. R. Canton-Vitoria, Dr. N. Tagmatarchis  
Theoretical and Physical Chemistry Institute  
National Hellenic Research Foundation  
48 Vassileos Constantinou Avenue, 11635, Athens (Greece)  
E-mail: rcanton@eie.gr  
tagmatar@eie.gr

[b] Dr. N. Heliopoulos  
700 Military Factory  
Supreme Military Support Command  
50 Anapfseos, 18648 Piraeus (Greece)

[c] Dr. N. Boukos  
Institute of Nanoscience and Nanotechnology  
National Centre for Scientific Research "Demokritos"  
Patriarchou Grigoriou E' & Neapoleos Str., 15341 Agia Paraskevi Attica (Greece)

[d] S. Vasilakos, D. Siamidis  
Siamidis S.A.  
Industrial Zone, Inofita 32011 Viotia (Greece)

[e] Dr. K. Stamatakis  
Institute of Biosciences and Applications  
National Center for Scientific Research "Demokritos"  
Patriarchou Grigoriou E' & Neapoleos Str., 15341 Agia Paraskevi Attica (Greece)

Supporting information for this article is available on the WWW under <https://doi.org/10.1002/chem.202301400>

This article is part of a joint Special Collection in honor of Maurizio Prato.

© 2023 The Authors. Chemistry - A European Journal published by Wiley-VCH GmbH. This is an open access article under the terms of the Creative Commons Attribution Non-Commercial NoDerivs License, which permits use and distribution in any medium, provided the original work is properly cited, the use is non-commercial and no modifications or adaptations are made.

25% enhancement of the tensile strength.<sup>[12]</sup> What is more, when Kevlar was subjected to a process of spin-spray-coating with CNTs, the conductivity of the fabric increased to 65 S/cm.<sup>[13]</sup> Conversely, the new functionalized nanomaterials with Kevlar have been used as additives to improve the properties of polymers. For example, mixtures of Kevlar with graphene nanoribbons<sup>[14]</sup> or with CNTs<sup>[15]</sup> were able to improve the tensile strength of PVC and polyvinyl acetate.<sup>[16]</sup> However, in all of those cases, non-covalent strategies such as  $\pi$ - $\pi$  stacking interactions and van der Waals forces were commonly employed for the modification of Kevlar, with major disadvantage being the uncontrollable release of the nanomaterial over time, lowering the efficacy of the modified fabric. This is especially important for clothing because physisorbed species are inevitably easily removed during continuous washings due to the mechanical movements of the washings and the detergents' capacity to eliminate any hydrophobic and hydrophilic adducts.

Relying on robust covalent techniques to functionalize Kevlar with nanomaterials, the chemistry at the *mer* units has been less explored and instead the terminal carboxylic acids or amines of oligomers or polymers of PPTA have been greatly used. In this context, copolymerization is without a doubt the most widely employed approach for increasing the number of functionalities of Kevlar.<sup>[17]</sup> For example, CNTs chemically modified with dimers of PPTA were mixed with monomers of Kevlar growing in-situ the fibers.<sup>[18]</sup> Although a similar strategy was described with graphene derivatives, we may highlight that graphene has 1 TPa in Young's modulus and 130 GPa in strength and is commonly combined with other materials.<sup>[19]</sup> In fact, graphene oxide was covalently functionalized with dimers of PPTA, enhancing the strength of Kevlar fibers by 30% at only 0.5% of mass weight.<sup>[20]</sup>

In essence, the chemical modification of Kevlar produces excellent outcomes. Nevertheless, altering the synthetic route of Kevlar is unappealing to textile industries, which have spent significant resources optimizing the fabric process to produce pure Kevlar, resulting in more convenient post-functionalization of Kevlar fabrics. However, post-functionalization methodologies are still at infancy and the functionalization loading is very small. Few techniques have been explored to increase the degree of covalent functionalization. For example, the polymeric PPTA chains of Kevlar break in small nanofibers during a hydrolysis process by NaOH,<sup>[21]</sup> KOH<sup>[22]</sup> or plasma treatment<sup>[23]</sup> and the resulting nanofibers are further employed in a wide range of applications such as water desalination, electrodes, or electrical-conductive membranes.<sup>[24]</sup> On the other hand, in some works the aromatic rings of the *mer* chains of PPTA were functionalized. Primarily, a mixture of sulfuric and nitric acid allows the introduction of nitro groups at the phenyl rings of PPTA<sup>[25]</sup> and subsequent reduction of the so-formed nitro groups yields free amines, which can increase the strength properties of Kevlar by 32% under very specific conditions.<sup>[26]</sup> In addition, hydrogens of the aromatic rings of PPTA can be exchanged by  $-\text{Br}$  or  $-\text{OH}$ , upon treatment with bromine<sup>[25]</sup> or phosphoric acid.<sup>[27]</sup> Next, sulfonyl azide derivatives allow the incorporation of sulfonyl units at the aromatic rings of Kevlar.<sup>[28]</sup> Similarly, chlorosulfonation introduces  $-\text{SO}_2\text{Cl}$  groups on the

aromatic rings of Kevlar, allowing further functionalization and increasing the number of free carboxylic acids, alkenes or amines on Kevlar.<sup>[26]</sup> Unfortunately, all those modifications involving sulfonyl derivatives decrease the mechanical properties of Kevlar, probably due to the size of  $-\text{SO}_2\text{Cl}$  that disrupts the strong bonding between PPTA polymer chains.<sup>[29]</sup> Finally, deprotonation of the amides in *mer* units of Kevlar allows the reaction with alkyl halogenides. Using the latter strategy, alkoxy silane groups have been attached onto Kevlar, enhancing the interlaminar shear strength in epoxy resins composites.<sup>[30]</sup>

Conversely, one of the most important aspects of graphene oxide (GO) is its antibacterial properties.<sup>[31,32]</sup> Briefly, two-dimensional nanomaterials can wrap around bacteria and their sharp edges have the potential to break microorganisms cell membranes. In addition, GO harms bacteria by promoting an oxidative stress process that results in the generation of reactive oxygen species.<sup>[31]</sup>

With all the above in mind and considering that often the characterization of covalent functionalization results spectroscopically difficult to assess and unclear, additional strategies involving the covalent post-functionalization of Kevlar fabrics must be developed. Furthermore, it is of utmost importance that the covalent post-functionalization of Kevlar does not occur at the expense of the other otherwise excellent mechanical properties of the fabric. Thus, the first objective of this contribution is to spectroscopically prove, step-by-step, the post-functionalization of Kevlar fabric and control the degree of functionalization. To this end, nitro groups were first introduced into Kevlar *mer* units and then reduced to the corresponding amines. Next, the addition of a linker enriches the loading of alkyl amines, which easily react with graphene oxide. Ideally, this strategy interconnects distant polymer chains and therefore enhances the mechanical properties of Kevlar. Raman spectroscopy and SEM imaging evidenced the post-functionalization of the fabric. Additionally, with the aid of IR, TGA and by performing Kaiser tests, the functionalization degree was monitored. Most importantly, when the hybrid fabric, in which GO nanosheets have been covalently incorporated onto the modified Kevlar, exposed to cyanobacterial *Synechococcus* we found that bacteria growth was fully inhibited, while the ultimate strength of the hybrid fabric enhanced by 20% compared to intact Kevlar. In short, the new covalently modified fabric can be used to create washable clothing with long lifespan and free of bacteria for longer periods of time.

## Results and Discussion

The synthetic route to functionalize Kevlar fabric with graphene oxide (GO) is shown in Figure 1. This is a multi-step sequence of reactions, in which the first step involves nitration of Kevlar, via immersion of the intact fibers in a mixture of nitric and sulfuric acid, to furnish nitro-Kevlar derivative **1**.<sup>[25]</sup> Next, reduction of the nitro-groups decorating the fabric with hydrazine/Raney-Ni yields amine-Kevlar derivative **2**.<sup>[26]</sup> When **2** was employed for the functionalization of GO, via the well-established methodology of in-situ generated aryl diazonium salts, unclear results

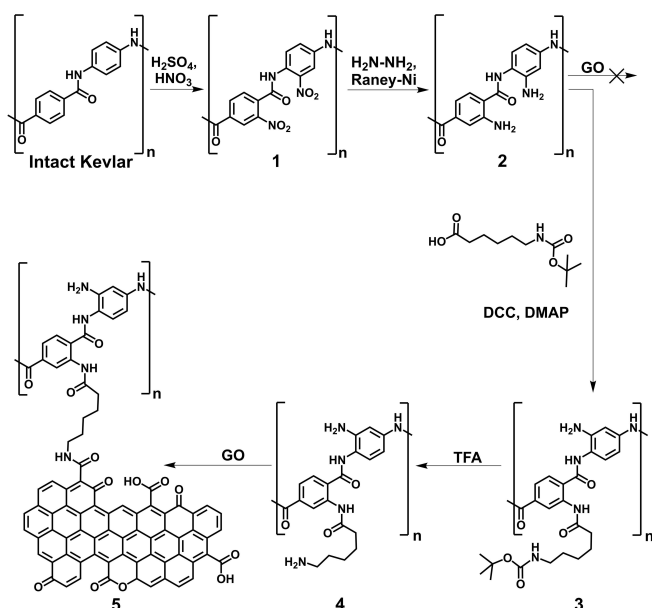


**Figure 1.** Functionalization scheme for modified Kevlar fabric en route to the realization of Kevlar-GO hybrid fabric 5.

were obtained, probably due to steric repulsions developed between the modified fabric and the graphene sheets. To overcome this hurdle, 6-(Boc-amino)caproic acid is employed to condense with amine-Kevlar derivative 2, yielding modified Kevlar fabric 3. Next, liberation of the free amine units, via acidic cleavage of the Boc moiety, furnishes derivative 4, in which the presence of the extended alkyl chain minimizes the steric repulsions between the amine-modified Kevlar 4 and GO. Finally, condensation reaction between amine-modified Kevlar 4 and the acyl chloride activated GO, yields the Kevlar-GO hybrid fabric 5.

Notably, macroscopic color alteration of the fabric, for example during nitration of intact Kevlar to modified fabric 1, from light green to maroon-brown, and further to light-brown, upon reduction to 2, suggests changes of the internal structure of Kevlar. Moreover, GO acts as pigment, further browning the fabric in Kevlar-GO hybrid 5 (Figure S1). In addition, to the first optical identification for the transformations occurred, complementary spectroscopic methods can conveniently monitor the changes during the various functionalization steps of Kevlar fabric. In this context, IR spectroscopy is the most essential technique employed to demonstrate the covalent functionalization of the fabric. Intact Kevlar shows characteristic signatures due to N–H stretching at  $3300\text{ cm}^{-1}$ , aromatic carbonyl amide and N–H bending vibrations at  $1650\text{ cm}^{-1}$  and  $1540\text{ cm}^{-1}$ , respectively.<sup>[33]</sup> Then, nitration of Kevlar, furnishing 1, is confirmed by the development of new N=O stretching bands at  $1490$  and  $1340\text{ cm}^{-1}$  (Figure 2). In addition, the aromatic carbonyl amide signatures of Kevlar are strongly blue-shifted to  $1665\text{ cm}^{-1}$  due to the electron accepting character of the incorporated  $-\text{NO}_2$  groups. Further, the absence of any carboxylic acid groups at  $1732\text{ cm}^{-1}$  (carbonyl) or  $3740\text{ cm}^{-1}$  (hydroxyl) ensures that the polymer chains of PPTA do not dissociate, contrasting earlier reported cases.<sup>[34,35]</sup> Reduction to 2 results in

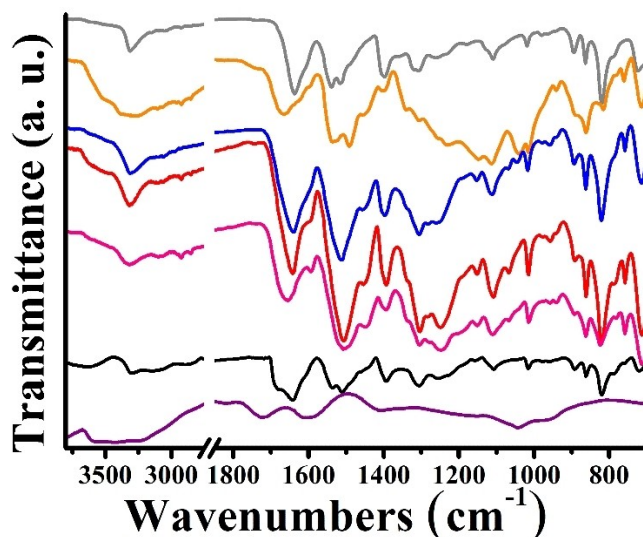


**Figure 2.** IR spectra for intact Kevlar (gray), modified fabric 1 (orange), 2 (blue), 3 (red), 4 (pink), Kevlar-GO hybrid fabric 5 (black), and GO (purple).

the disappearance of the  $-\text{NO}_2$  signatures, followed by an alteration in the morphology of the N–H band at  $3321\text{ cm}^{-1}$ . The electron donating character of amines present at the aromatic rings of Kevlar fabric induces an additional change at the carbonyl amide band, appearing at  $1634\text{ cm}^{-1}$  in amine-Kevlar 2. Next, the presence of aliphatic C–H vibrations at  $2912\text{ cm}^{-1}$  ensures the successful incorporation of the Boc alkyl chain in modified fabric 3. Further, widening of the amine vibration at  $3322\text{ cm}^{-1}$  and shift of the carbonyl amide vibration to  $1655\text{ cm}^{-1}$  ensures the cleavage of Boc in modified fabric 4. Finally, covalent incorporation of GO sheets onto the Kevlar fabric results in the development of a new aliphatic carbonyl amide band at  $1687\text{ cm}^{-1}$ , while the decrement of the band due to carboxylic acid moieties of GO (i.e. originally appearing at  $1727\text{ cm}^{-1}$  in GO) further validates the successful formation of Kevlar-GO hybrid fabric 5.

Raman spectroscopy also provides relevant information about the internal structure of Kevlar. Upon  $514\text{ nm}$  excitation, Figure 3a shows the signatures of the fabric, namely at  $1277$ ,  $1327$  and  $1515\text{ cm}^{-1}$ , associated to C–C vibrations, at  $1318\text{ cm}^{-1}$  associated to C–H in-plane vibrations, at  $1648\text{ cm}^{-1}$  corresponding to amide vibrations and the stronger band at  $1611\text{ cm}^{-1}$  associated to C–C aromatic ring stretching vibrations.<sup>[36]</sup> Nitration of the fabric yielding 1 produces a red shift of the C–C aromatic ring vibrations, displacing the signature until  $1609\text{ cm}^{-1}$ . The electron donating character of the amine groups in 2 produces the opposite effect, shifting to the blue the signatures back to  $1611\text{ cm}^{-1}$ . The same trend is observed in the Raman spectrum of modified fabric 3 (Figure 3b), while no further appreciable spectral changes are observed in 4. The aforementioned Raman spectral shift between intact Kevlar and modified fabrics 1–4 are homogeneous in nature, evidenced by spectral mapping assays (Figure 3c). Finally, Raman spectral signatures of GO, namely D and G bands at  $1344$  and  $1592\text{ cm}^{-1}$ , respectively, are easily identified in the Kevlar-GO

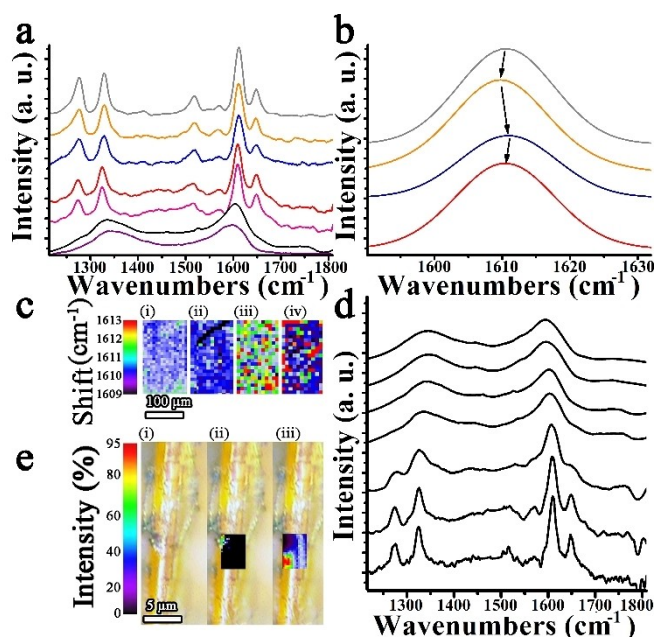


**Figure 3.** a) Raman spectra (514 nm) for intact Kevlar (gray), modified fabric 1 (orange), 2 (blue), 3 (red), 4 (pink), Kevlar-GO hybrid fabric 5 (black) and GO (purple). b) Raman spectral shift of the aromatic band at  $1610\text{ cm}^{-1}$  for intact Kevlar (gray), modified fabric 1 (orange), 2 (blue) and 3 (red). c) Spectral mapping shift of the C–C aromatic band at  $1610\text{ cm}^{-1}$  for intact Kevlar (i), modified fabric 1 (ii), 2 (iii) and 3 (iv). d) Raman spectral position dependence of Kevlar-GO hybrid fabric 5, where the length between each spectrum was 250 nm. e) Optical microscope images for Kevlar-GO hybrid fabric 5 showing (i) rich areas of GO (gray) and Kevlar (orange-yellow), (ii) Raman spectral map intensity of the G-band for GO, and (iii) Raman spectral map of Kevlar.

hybrid fabric 5. The fluctuation of the Raman spectra across distance is shown in Figure 3d and e, demonstrating that a simple micron distance is sufficient to switch from a very rich region of GO to another one in which Kevlar signatures are predominant, implying that massive non-covalent aggregations of GO are missing in the Kevlar-GO hybrid fabric 5.

The thermal stability of the modified fabrics was assessed by TGA. Intact Kevlar is thermally stable up to  $530\text{ }^{\circ}\text{C}$ , while at the temperature range  $530\text{--}615\text{ }^{\circ}\text{C}$  the amide bonds of Kevlar degrade.<sup>[9]</sup> Incorporation of  $-\text{NO}_2$  groups in the *mer* units of Kevlar reduces the global thermal stability of 1, resulting in the decomposition of  $\text{NO}_2$  groups as well as all the polymeric chains that were perturbed by interactions of the new functionalities. On the other hand, the presence of the amine groups in 2 results in the thermal disintegration of the modified fabric at  $360\text{--}430\text{ }^{\circ}\text{C}$ , regaining some of the thermal stability<sup>[26]</sup> of the polymer chains (Figure 4a). The loading of the alkyl organic linker in the modified fabric results in a small thermal decomposition of the alkyl organic chain up to  $275\text{ }^{\circ}\text{C}$ , enhancing the mass loss from 2.0 in 2 to 3.0 and 2.5% in 3 and 4, respectively. In accordance with the atomic mass, both modified fabrics 3 and 4 show 1 functional group per every 94-*mer* units of Kevlar. Finally, incorporation of GO onto the fabric in 5 results in an enhancement of the mass loss, i.e. 30%, up to  $400\text{ }^{\circ}\text{C}$ , due to the degradation of oxygen species present on GO. Noteworthy, the robust covalent immobilization of GO onto

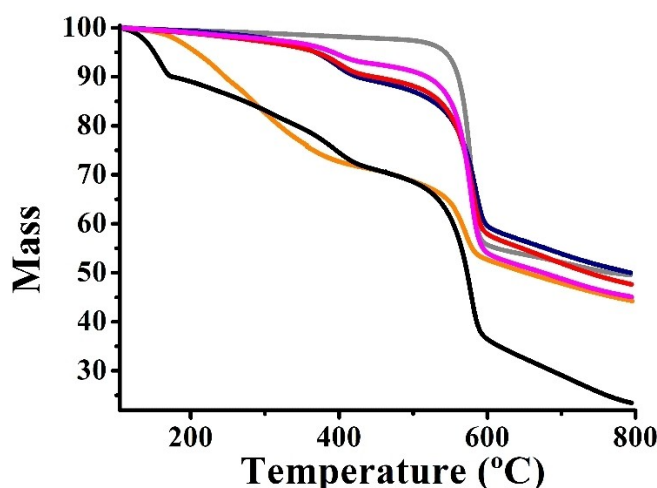


**Figure 4.** TGA graphs for intact Kevlar (gray), modified fabric 1 (orange), 2 (blue), 3 (red), and 4 (pink), and Kevlar-GO hybrid fabric 5 (black), obtained under inert nitrogen atmosphere.

the modified Kevlar fabric, is further supported by the Kaiser test, since the  $83\text{ }\mu\text{mol}/\text{cm}^2$  of aliphatic amines in 4 were found reduced to only  $9\text{ }\mu\text{mol}/\text{cm}^2$  in Kevlar-GO hybrid fabric 5.

Scanning electron microscopy (SEM) imaging was employed to evaluate the morphology of Kevlar-GO hybrid fabric 5. Intact Kevlar exhibits well defined aligned fibers of  $10\text{ }\mu\text{m}$  (Figure 5a and b), whereas when graphene oxide is covalently incorporated it collects and wraps multiple micro-fibers (Figure 5c and d). Interestingly, the microfibers of Kevlar-GO fabric 5 appear to be intact, with no signs of deterioration or shape alteration. Furthermore, SEM imaging suggests that the incorporation of GO was occurred on the surface of the modified Kevlar fibers, without appreciable intercalation, totally covering and shielding the fiber from external hazards, while at the same time it

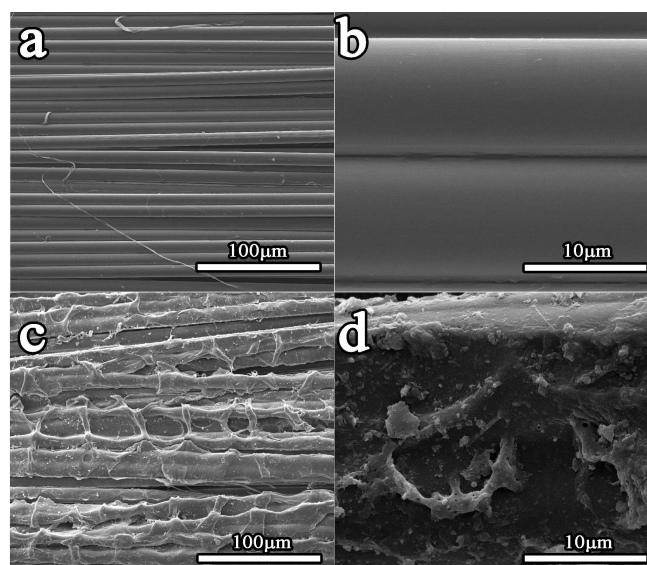


**Figure 5.** SEM images of (a, b) intact Kevlar, and (c, d) Kevlar-GO hybrid fabric 5.

enhances the interconnectivity of the fibers. Similar coverage was reported by SEM imaging in non-covalently functionalized Kevlar nanofibers with 1.75 % carbon nanotube,<sup>[12]</sup> which can be well compared to the 2.7 % GO content in the current Kevlar-GO hybrid fabric 5 (see below), suggesting a beneficial influence on mechanical properties.

At this stage, the modification of Kevlar fabric as well as its hybridization with graphene has been adequately evidenced. Next, we focus on controlling the level of functionalization, which is exclusively governed by controlling the time of the nitration of Kevlar. A set of nitration reactions at varied periods was performed, i.e. at 10, 20, 40, 80, 160, and 300 seconds, and the product was subsequently assessed by TGA, IR and Kaiser test (Figure S2-S4). In short, increasing the nitration reaction time of intact Kevlar enhances the changes previously discussed, cf. Figure 2 and 4. For example, TGA indicates an increase in the thermal degradation of Kevlar fibers in 1, by registering 10, 11, 13, 20, and 27 % mass loss at 400 °C, during nitration periods of 10, 20, 40 or 300 seconds (Figure S2a), respectively. Reduction of the -NO<sub>2</sub> group to -NH<sub>2</sub> in 2, results in a mass loss of 4.5, 5.0, 7.5, and 10.5 %, respectively, at 430 °C (Figure S2b). The presence of the organic chain in 3 attributes to a further small loading in the fabric, which, however, is handicapped by the limit of detection of our instrument. Nevertheless, at 160 and 300 seconds of nitration of Kevlar, TGA shows a mass loss of 2.4 and 2.9 % in 3, which decreases to 1.7 and 2.2 %, respectively, in 4 (Figure S2c and d). Finally, the Kevlar-GO hybrid fabric 5 shows a degradation of oxygen species mainly due to the presence of GO (Figure S2e) at the range 100–400 °C. For example, the mass loss between 10 and 80 seconds range between 2 and 8 % enhancing at 160 and 300 seconds up to 12 and 25 %, respectively. On the other hand, the Kaiser test (Figure S4) shows 3, 9, 15, 30, 40 and 60 μmol/cm<sup>2</sup> of free amines in 4 at 10, 20, 40, 80, 160 and 300 seconds of nitration reaction of Kevlar, i.e. the first step in the multi-sequence organic transformations. Those Kaiser test values in 4 have a linear relationship between the amine loading and the logarithmic of nitration time exposed the intact Kevlar fabric. Then, the amine loading decreases in Kevlar-GO hybrid fabric 5, as expected, to 1.0, 3.0, 0.6, 1.0, 2.0 and 4.0 μmol/cm<sup>2</sup>, respectively.

In fact, controlling the level of covalent functionalization on Kevlar fibers is extremely interesting, since addition to new functionalities gradually disrupts the structure of the polymer and their intrinsic properties. For example, the fiber of Kevlar fabric breaks at ultimate strength of 1.090 GPa and this value decreases to 0.532, 0.530, 0.282, 0.221, 0.141 and 0.082 GPa after 10, 20, 40, 80, 160, and 300 seconds of nitration treatment, respectively, yielding 1. However, the strength improves after reduction of 1<sup>[26]</sup> and further amidation of so-formed 2 yielding 3. For example at 10 seconds, the strength of the fiber increases from 0.532 GPa in 1 to 0.603 GPa in 2 and 0.607 GPa in 3. After cleavage of Boc, the subsequent liberation of free amines produces new hydrogen bonds in 4, interconnecting different polymer chains within the fibers of Kevlar and this is highlighted as the strength of the modified fiber increases to 1.001, 0.742, 0.730, 0.600 and 0.177 GPa in 4 when considering initial

nitration reactions at 10, 20, 40, 80 and 160 seconds, respectively. Moreover, we can preserve more than 90 % of the strength of the intact Kevlar fabric. Covalent incorporation of GO within modified Kevlar in 5 interconnects the fibers towards amide bonds, which results in an additional increment of the ultimate strength of the hybrid fabric, breaking at 1.126, 1.312, 0.879, 0.636, 0.236 and 0.118 GPa, at initial nitration times of 10, 20, 40, 80, 160 and 300 seconds. It is noteworthy that especially at 10 and 20 seconds of nitration of intact Kevlar, we registered an improvement of the ultimate strength in hybrid fabric 5 of 3 and 20 %, respectively.

Finally, an innovative approach<sup>[37,38]</sup> was employed to assess the antibacterial properties of Kevlar-GO hybrid fabric 5, based on the different loading of GO onto Kevlar i.e. according to the different nitration periods employed in the first reaction of the multistep synthetic process shown in Figure 1. The value of the cyanobacterial *Synechococcus* colony proliferation ( $F_0$ ) in each Kevlar-GO hybrid fabric 5 was recorded every 24 h for a period of seven days. Then, the variation of the fluorescence intensity ( $M_t$ ), calculated according to Equation (1), is directly correlated with the antibacterial properties of the samples. In further depth, the ability of cyanobacterial cells to proliferate leads to an increase in chlorophyll (Chl)  $\alpha$  fluorescence intensity, while when the cells die, Chl  $\alpha$  breakdown begins and the fluorescence intensity falls. Figure 6 shows lower  $M_t$  values of Kevlar-GO hybrid fabric 5 at nitration time of 10 and 20 seconds as compared to intact Kevlar, which indicates an inhibition of *Synechococcus* cell proliferation. On the other hand, negative  $M_t$  values, at nitration time of 40–1200 seconds, ensure a reduction of the initial bacterial population of the colony (52.0 μg/mL) dropped on the fabric.<sup>[39–41]</sup> Overall, Figure 6 demonstrates substantially better antibacterial behaviour for Kevlar-GO hybrid fabrics 5 compared to intact Kevlar due to the covalent incorporation of GO nanosheets. Furthermore, Equation (2) allows to calculate the Bacterial Protection Index (BPI) after 7 days ( $II_7$ ) of Kevlar-GO hybrid fabric 5 at all the examined

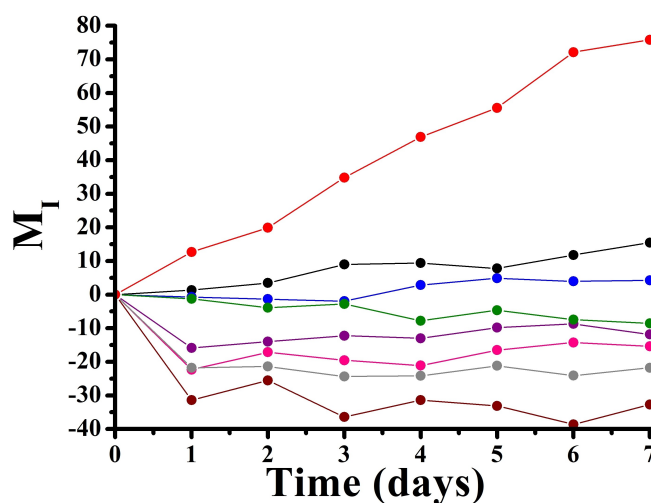


**Figure 6.**  $M_t$  evolution curves of cyanobacteria *Synechococcus* on intact Kevlar fabric (red) compared with Kevlar-GO hybrid fabric 5 with different nitration time upon upon 10s (black), 20s (blue), 40s (green), 80s (purple), 160s (pink) 300s (gray) and 1200 sec (wine) nitration reaction time.

nitration times and the values are further collected in Table 1. In short, under increasing nitration times, and consequently higher loading of GO onto modified Kevlar fabric, the  $\Pi_7$  improves, becoming the fabric totally protected at nitration times of 40 seconds or higher, whereas the  $\Pi_7$  value at 20 seconds is still remarkable.

$$M_i = \frac{F_{0i} - F_{00}}{F_{00}} \times 100 \quad (1)$$

$$\Pi_7 = \frac{M_{U_7} - M_{T_7}}{M_{U_7}} \times 100 \quad (2)$$

Where  $F_{00}$  is the value of Chl  $\alpha$  fluorescence of cyanobacterium at zero contact time and  $F_{0i}$  is the value of Chl  $\alpha$  fluorescence of cyanobacterium after 1, 2, ...,  $i$  days.  $M_{U_7}$  and  $M_{T_7}$  are the change in cyanobacterial Chl  $\alpha$   $F_0$  value after seven days of incubation at intact Kevlar and Kevlar-GO hybrid fabric 5, respectively.<sup>[37]</sup>

## Conclusions

An easy and straightforward strategy to post-functionalize fabrics of Kevlar, featuring alkyl amines covalently connected with the aromatic rings of *mer* units of PPTA chains that can further condense with carboxylic acids of GO, is presented. We fully prove via spectroscopic means each step of the covalent functionalization of Kevlar en route the realization of Kevlar-GO hybrid fabric 5 and importantly we showcase a methodology to control the loading of the organic addends and eventually the presence of GO, monitored by TGA, Kaiser test and IR, to preserve the unique mechanical strength of the fabric. Moreover, we registered an improvement of 20% of the ultimate strength of the modified Kevlar covalently hybridized with GO nanosheets under low functionalization degree. Notably, at optimal strength the Kevlar-GO hybrid fabric 5 showed a 94.4% reduction of the cyanobacterial *Synechococcus* cell proliferation.

**Table 1.** Loading of GO onto modified Kevlar fabric by TGA, ultimate strength, and bacterial protection index (BPI) after 7 days ( $\Pi_7$ ) for hybrid fabric 5 based on varied nitration time of intact Kevlar.

Nitration time <sup>[a]</sup> [s]	GO loading [%] <sup>[b]</sup>	Strength [GPa]	$\Pi_7$ <sup>[c]</sup>
Intact kevlar	0	1.090 ± 0.030	0.0
10	2.0	1.126 ± 0.028	79.6
20	2.7	1.312 ± 0.028	94.4
40	2.9	0.879 ± 0.027	111.3
80	8.0	0.636 ± 0.030	115.6
160	12	0.236 ± 0.012	120.2
300	25	0.118 ± 0.015	128.7
1200	30	0.050 ± 0.033	143.1

[a] The first step in the multi-sequence organic transformations for obtaining hybrid fabric 5. [b] Based on TGA. [c] The estimated  $\Pi_7$  values corresponds to total antibacterial activity and the value above 100 demonstrates the same protection as that of 100.

Even though we have not optimized the reported process for commercial uses, we firmly believe that it can be applied in that field. For instance, well-established, inexpensive techniques such as nitration, reduction to amine, and further amidation reactions are frequently employed in industrial processes. In addition, we find the basis for monitoring the fabric's chemical transformations by employing very fast and straightforward techniques such as IR, TGA or Kaiser test. Hence, the reported strategy holds scalability promises. We are confident that the current methodology not only can be extended to other aramid fibers, but also opens a new route for accurate covalent functionalization of Kevlar with a broad range of nanomaterials.

## Experimental Section

**Nitro-Kevlar 1:** 100 mL of H<sub>2</sub>SO<sub>4</sub> (96%) was mixed with 10 mL of nitric acid (65%) in an ice bath for 10 min. Then, 5 cm × 5 cm Kevlar fibers were immersed for different times (10, 20, 40, 80, 160 and 300 sec; optimal conditions 20 sec) under stirring. After this period, the fiber was quickly removed from the acid solution and immersed in 300 mL of cold water, followed by extensive washing with water at room temperature and then with acetone. Edges of nitro-modified Kevlar 1 were overoxidized and removed.

**Amine-Kevlar 2:** Nitro-modified Kevlar 1 fabric fibers were immersed in 200 mL of methanol. Then, few spoons (1-2 g) of Raney-Ni were added to the solution while stirring. After some sonication, 10 mL of hydrazine was added and the reaction mixture was stirred for 48 h. During this time, small portions of hydrazine were added, every time bubbles on the solution stopped forming. After that period, the modified amine-modified Kevlar 2 fabric was removed from the methanol solution and extensively washed with water at room temperature and then with acetone.

**Boc-Kevlar 3:** Amine-modified Kevlar 2 fabric fibers were immersed in dry dichloromethane containing 30 mg of dry molecular sieves 4 A. Then, 1 g of 6-Boc-aminocaproic acid and 3 equivalents of HOBT was added and sonicated for 5 min. Then, 3 equivalents of DCC were added and the reaction mixture was stirred at 50 °C for 2 days. Afterwards, the Boc-modified Kevlar 3 was extensively washed with water, methanol and acetone.

**Amine-Kevlar 4.** Boc-modified Kevlar 3 fabric fibers were immersed in 50 mL of a mixed solution of dichloromethane and trifluoroacetic acid (90/10 v/v) at room temperature. The mixture was sonicated for 15 min and stirred overnight. Afterwards, the amine-modified Kevlar 4 was extensively washed with water, methanol and acetone.

**Kevlar-GO hybrid fabric 5:** 100 mg of graphene oxide and 30 mg of dry molecular sieves 4 A in 100 mL of a SOCl<sub>2</sub>/DMF (50/50 v/v) solution were sonicated for 1 h and heated under stirring for 18 h at 75 °C. Then, the excess of SOCl<sub>2</sub> was removed under vacuum and the amine-modified Kevlar 4 was placed into the reaction mixture. The reaction was kept at 50 °C and stirred for 2 days. Afterwards, the Kevlar-GO hybrid fabric 5 was extensively washed with water, methanol, and acetone.

## Supporting Information

Experimental section, synthetic routes and additional spectroscopic and thermal characterization data are shown at the

Supporting Information. The authors have cited additional references within the Supporting Information [42,43].

## Acknowledgements

Financial support by the European Regional Development Fund of the European Union and Greek national funds through the Operational Program Competitiveness, Entrepreneurship, and Innovation, under the call RESEARCH-CREATE-INNOVATE (project code: T2EDK-01316) is acknowledged.

## Conflict of Interests

The authors declare no conflict of interest.

## Data Availability Statement

The data that support the findings of this study are available from the corresponding author upon reasonable request.

**Keywords:** antibacterial properties · fabric · graphene · kevlar · nanosheets

- [1] K. Hillermeier, *Text. Res. J.* **1984**, *54*, 575–580.
- [2] L. Liu, Z. Li, Q. Che, *ACS Appl. Nano Mater.* **2019**, *2*, 2160–216.
- [3] J. Lyu, Z. Liu, X. Wu, G. Li, D. Fang, X. Zhang, *ACS Nano* **2019**, *13*, 2236–2245.
- [4] A. D. Roberts, P. Kelly, J. Bain, J. J. Morrison, I. Wimpenny, M. Barrow, R. T. Woodward, M. Gresil, C. Blanford, S. Hay, J. J. Blaker, S. G. Yeates, N. S. Scrutton, *Chem. Commun.* **2019**, *55*, 11703–1170.
- [5] L. Lev, X. Han, L. Zong, M. Li, J. You, X. Wu, C. Li, *ACS Nano* **2017**, *11*, 8178–8184.
- [6] D. Tanner, J. A. Fitzgerald, B. R. Phillips, *Angew. Chem. Int. Ed.* **1989**, *28*, 649–654.
- [7] H. Chae, S. Kumar, *J. Appl. Polym. Sci.* **2006**, *100*, 791–802.
- [8] P. L. Walton, A. J. Majumdar, *J. Mater. Sci.* **1983**, *18*, 2939–2946.
- [9] X. Liu, W. Yu, *J. Appl. Polym. Sci.* **2005**, *99*, 937–944.
- [10] F. Wang, Y. Wu, Y. Huang, *Composites Part A* **2018**, *110*, 126–13.
- [11] I. K. Sideri, N. Tagmatarchis, *Mater. Horiz.* **2021**, *8*, 3187–3200.
- [12] I. O'Connor, H. Hayden, J. N. Coleman, Y. K. Gun'ko, *Small* **2009**, *5*, 466–469.
- [13] B. K. Little, Y. Li, V. Cammarata, R. Broughton, G. Mills, *ACS Appl. Mater. Interfaces* **2011**, *3*, 1965–1973.
- [14] M. Lian, J. Fan, Z. Shi, H. Li, J. Yin, *Polymer* **2014**, *55*, 2578–2587.
- [15] I. O'Connor, H. Hayden, S. O'Connor, J. N. Coleman, Y. K. Gun'ko, *J. Mater. Chem.* **2008**, *18*, 5585–5588.
- [16] I. O'Connor, H. Hayden, S. O'Connor, J. N. Coleman, Y. K. Gun'ko, *J. Phys. Chem. C* **2009**, *113*(47), 20184–20192.
- [17] J. A. Reglero-Ruiz, M. Trigo-López, F. C. García, J. M. García, *Polymer* **2017**, *9*, 414.
- [18] T. Sainsbury, K. Erickson, D. Okawa, C. S. Zonte, J. M. Fréchet, A. Zettl, *Chem. Mater.* **2010**, *22*, 2164–2171.
- [19] A. Stergiou, R. Cantón-Vitoria, M. N. Psarrou, S. P. Economopoulos, N. Tagmatarchis, *Prog. Mater. Sci.* **2020**, *114*, 100683.
- [20] Y. Wang, Z. X. Shi, J. Yin, *Polymer* **2011**, *16*, 3661–3670.
- [21] T. M. Akshat, S. Misra, M. Y. Gudiyawar, J. Salacova, M. Petru, *Fibers Polym.* **2019**, *20*, 991–1002.
- [22] Z. Zhang, S. Yang, P. Zhang, J. Zhang, G. Chen, X. Feng, *Nat. Commun.* **2019**, *10*, 2920.
- [23] Q. Wang, S. Kaliaguine, A. Ait-Kadi, *J. Appl. Polym. Sci.* **1993**, *48*, 121–136.
- [24] Y. Zhao, X. Li, J. Shen, C. Gao, B. Van der Bruggen, *J. Mater. Chem. A* **2020**, *8*, 7548–7568.
- [25] Y. Wu, G. C. Tesoro, *J. Appl. Polym. Sci.* **1986**, *31*, 1041–1059.
- [26] R. Benrashid, G. C. Tesoro, *Text. Res. J.* **1990**, *60*, 334–344.
- [27] G. Li, C. Zhang, Y. Wang, P. Li, Y. Yu, X. Jia, H. Liu, X. Yang, Z. Xue, S. Ryu, *Compos. Sci. Technol.* **2008**, *68*, 3208–3214.
- [28] J. Yatvin, S. A. Sherman, S. F. Filocamo, J. Locklin, *Polym. Chem.* **2015**, *6*, 3090–3097.
- [29] T. K. Lin, B. H. Kuo, S. S. Shyu, S. H. Hsiao, *J. Adhesion Sci. Technol.* **1999**, *13*, 545–560.
- [30] T. Ai, R. Wang, W. Zhou, *Polym. Compos.* **2007**, *28*, 412–416.
- [31] I. M. Ida, S. Shamsi, *Int. J. Mol. Sci.* **2022**, *23*, 9096.
- [32] E. B. Masoudipour, S. Kashanian, N. Maleki, *Chem. Phys. Lett.* **2017**, *668*, 56–63.
- [33] M. Mukherjee, S. Kumar, S. Bose, C. K. Das, A. P. Kharitonov, *Polym. Plast. Technol.* **2008**, *47*, 623–629.
- [34] C. Arrieta, É. David, P. Dolez, T. Vu-Khanh, *Polym. Degrad. Stab.* **2011**, *96*, 1411–1419.
- [35] N. Ramasamy, V. Arumugam, S. Rajkumar, *Bull. Mater. Sci.* **2019**, *42*, 173.
- [36] G. Washer, T. Brooks, R. Saulsberry, *J. Mater. Civ. Eng.* **2009**, *21*, 226–234.
- [37] N. S. Heliopoulos, A. Galeou, S. K. Papageorgiou, E. P. Favvas, F. K. Katsaros, K. Stamatakis, *J. Microbiol. Methods* **2015**, *112*, 49–54.
- [38] N. S. Heliopoulos, A. Galeou, S. K. Papageorgiou, E. P. Favvas, F. K. Katsaros, K. Stamatakis, *J. Microbiol. Methods* **2016**, *121*, 1–4.
- [39] K. Ellinas, D. Kefallinou, K. Stamatakis, E. Gogolides, A. Tserepi, *ACS Appl. Mater. Interfaces* **2017**, *9*, 39781–39789.
- [40] D. Kefallinou, K. Ellinas, Th. Speliotis, K. Stamatakis, E. Gogolides, A. Tserepi, *Coating* **2019**, *10*, 25.
- [41] N. S. Heliopoulos, G. N. Kouzilos, A. I. Giarmenitis, S. K. Papageorgiou, K. Stamatakis, F. K. Katsaros, *Fibers Polym.* **2020**, *21*, 1238–1250.[42] R. Y. Stanier, J. Deruelles, R. Rippka, M. Herdman, J. B. Waterbury, *Microbiology* **1979**, *111*, 1–61.[43] P. Moran P, *Plant Physiology* **1982**, *69*, 1376–1381.

Manuscript received: May 2, 2023

Accepted manuscript online: June 28, 2023

Version of record online: August 11, 2023